

The high power impulse magnetron sputtering discharge: An ionization region model study

Jón Tómas Guðmundsson^{1,2}

¹Department of Space and Plasma Physics,

KTH Royal Institute of Technology, Stockholm, Sweden

² Science Institute, University of Iceland, Reykjavik, Iceland

Departamento de Física - Centro de Ciências Tecnológicas

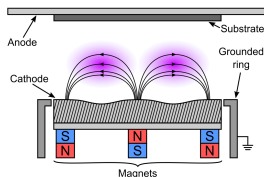
Universidade do Estado de Santa Catarina - UDESC

November 10., 2020



Introduction

- Magnetron sputtering discharges are widely used for thin film processing – spanning various industries
 - In the planar circular configuration it is simply a diode discharge with two concentric stationary cylindrical magnets placed directly behind the cathode target
-
- Applications include deposition of
 - thin films in integrated circuits
 - magnetic material
 - hard, protective, and wear resistant coatings
 - optical coatings
 - decorative coatings
 - low friction films

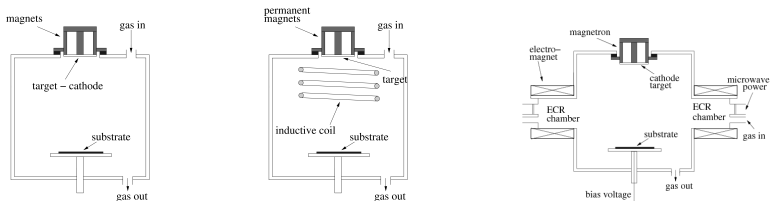


Gudmundsson and Lundin (2020) in High Power Impulse

Magnetron Sputtering Discharge, Elsevier, 2020



Introduction

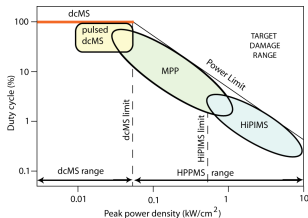


From Gudmundsson (2008) J. Phys.: Conf. Ser. **100** 082002

- A typical dc planar magnetron discharge operates at a pressure of 1 – 10 mTorr with a magnetic field strength of 10 – 50 mT and at cathode potentials 300 – 700 V
- Electron density in the substrate vicinity is in the range $10^{15} - 10^{16} \text{ m}^{-3}$
 - low fraction of the sputtered material is ionized ($\sim 1\%$)
 - the majority of ions are the ions of the inert gas
 - additional ionization by a secondary discharge (rf or microwave)

Introduction

- High ionization of sputtered material requires very high density plasma
- In a conventional dc magnetron sputtering discharge the power density (plasma density) is limited by the thermal load on the target
- High power pulsed magnetron sputtering (HPPMS)
- In a HiPIMS discharge a high power pulse is supplied for a short period
 - low frequency
 - low duty cycle
 - low average power

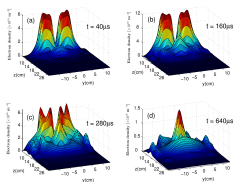


Gudmundsson et al. (2012) JVSTA **30** 030801

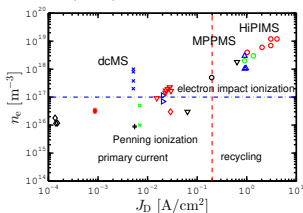
- Power density limits
 - $p_t = 0.05 \text{ kW/cm}^2$ dcMS limit
 - $p_t = 0.5 \text{ kW/cm}^2$ HiPIMS limit

Introduction

- Temporal and spatial variation of the electron density in HiPIMS discharge
- Ar discharge at 20 mTorr, Ti target, pulse length 100 μs
- The electron density in the substrate vicinity is of the order of $10^{18} - 10^{19} \text{ m}^{-3}$
- The electron density versus the discharge current density measured in dc diode and magnetron sputtering discharges



Bohlmark et al. (2005), IEEE Trans. Plasma Sci. **33** 346

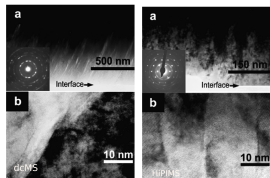


From Gudmundsson (2020) PSST **29** in press

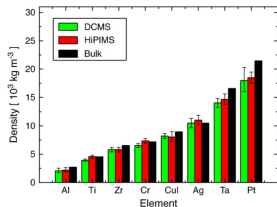
Thin film deposition



Thin film deposition – Fraction of ionization



Alami et al. (2005) JVSTA 23 278

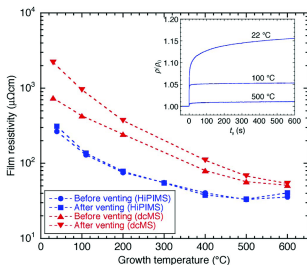


- In HiPIMS deposition, the high fraction of ionization of the sputtered species has been shown to lead to
 - the growth of smooth and dense films
 - enable control over their phase composition and microstructure
 - enhance mechanical, electrical, and optical properties
 - improve film adhesion
 - enable deposition of uniform films on complex-shaped substrates
- The mass density is always higher and the surfaces are significantly smoother when depositing with HiPIMS compared to dcMS at the same average power

From Samuelsson et al. (2010) SCT 202 591

Thin film deposition – Film Resistivity

- TiN as diffusion barriers for copper and aluminum interconnects
- HiPIMS deposited films have significantly lower resistivity than dcMS deposited films on SiO₂ at all growth temperatures due to reduced grain boundary scattering
- Thus, ultrathin continuous TiN films with superior electrical characteristics and high resistance towards oxidation can be obtained with HiPIMS at reduced temperatures

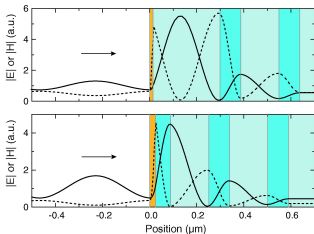


From Magnus et al. (2012) IEEE EDL **33** 1045

Thin film deposition – Bragg mirror

- Multilayer structures containing a high-contrast ($\text{TiO}_2/\text{SiO}_2$) Bragg mirror
- fabricated on fused-silica substrates
 - reactive HiPIMS TiO_2 (88 nm)
 - reactive dcMS SiO_2 (163 nm)
 - capped with semitransparent gold
- Rutile TiO_2 ($n = 2.59$) and SiO_2 ($n = 1.45$) provide a large index contrast
- Smooth rutile TiO_2 films can be obtained by HiPIMS at relatively low growth temperatures, without post-annealing

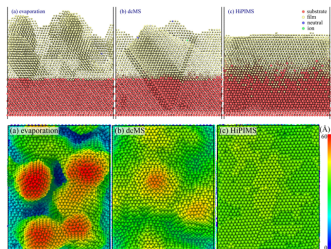
Agnarsson et al. (2013) TSF 545 445



From Leosson et al. (2012) Opt. Lett. **37** 4026

Thin film deposition – Molecular Dynamics simulation

- The effect of ionization fraction on the epitaxial growth of Cu film on Cu(111) substrate explored using Molecular Dynamics simulation
- Three deposition methods
 - thermal evaporation, fully neutral
 - dcMS, 50 % ionized
 - HiPIMS, 100 % ionized
- Higher ionization fraction of the deposition flux leads to smoother surfaces by two major mechanisms
 - decreasing clustering in the vapor phase
 - bicollision of high energy ions at the film surface that prevents island growth to become dominant

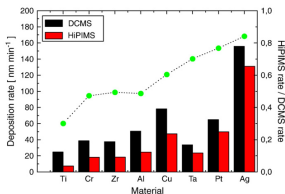


After Kateb et al. (2019) JVSTA **37** 031306



Thin film deposition – Deposition rate

- There is a drawback
- The deposition rate is lower for HiPIMS when compared to dcMS operated at the same average power
- The HiPIMS deposition rates are typically in the range of 30 – 85% of the dcMS rates depending on target material
- Many of the ions of the target material are attracted back to the target surface by the cathode potential



From Samuelsson et al. (2010) SCT **202** 591

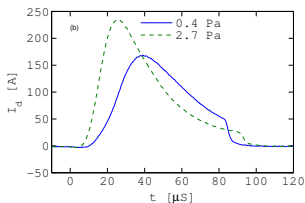
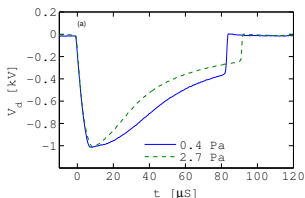
Voltage - Current - Time characteristics

Non-reactive HiPIMS



HiPIMS - Voltage - Current - time

- To describe the discharge current-voltage characteristics the current-voltage-time space is required
- The early work on HiPIMS used 50 – 100 μs pulses and a pulse repetition frequency in the range 50–1000 Hz
- The applied target voltage V_d and target current I_d for an argon discharge at 0.4 and 2.7 Pa. The target is made of copper 150 mm in diameter

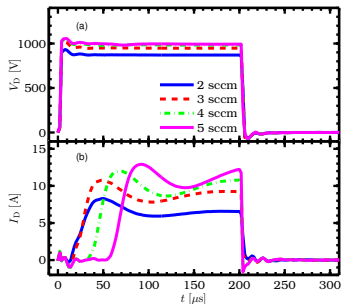


From Gudmundsson et al. (2012) JVSTA 30 030801



HiPIMS - Voltage - Current - time

- Modern pulser units have large storage capacitor, the voltage pulse V_D on the cathode can be almost square even for high currents I_D during the full pulse length
- A square voltage pulse is achieved as seen in the discharge voltage and current waveforms for Ar/N₂ discharges, with vanadium target, operated at different nitrogen flow rates while the argon flow rate was kept fixed at 40 sccm to achieve 0.9 Pa and 150 W average power for 200 μ s pulses



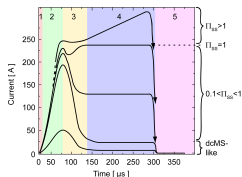
From Hajihoseini and Gudmundsson

(2017) JPD **50** 505302

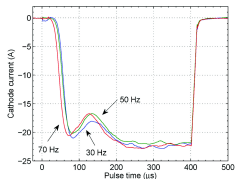


HiPIMS - Voltage - Current - time

- In a **non-reactive** discharge the current waveform shows an initial pressure dependent peak that is followed by a second phase that is power and material dependent
- The initial phase has a contribution from the working gas ions, whereas the later phase has a strong contribution from self-sputtering at high voltage



From Gudmundsson et al. (2012) JVSTA **30** 030801



From Magnus et al. (2011) JAP **110** 083306

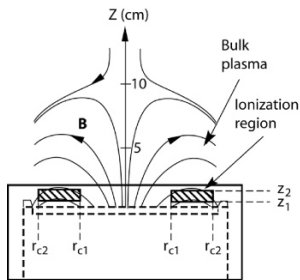


Ionization region model studies of non-reactive HiPIMS



Ionization region model non-reactive HiPIMS

- The ionization region model (IRM) was developed to improve the understanding of the plasma behaviour during a HiPIMS pulse and the afterglow
- The main feature of the model is that an ionization region (IR) is defined next to the race track
- The IR is defined as an annular cylinder with outer radii r_{c2} , inner radii r_{c1} and length $L = z_2 - z_1$, extends from z_1 to z_2 axially away from the target



The definition of the volume covered by the IRM

From Raadu et al. (2011) PSST 20 065007

Ionization region model non-reactive HiPIMS

- The temporal development is defined by a set of ordinary differential equations giving the first time derivatives of
 - the electron energy
 - the particle densities for all the particles
- The species assumed in the non-reactive-IRM are
 - cold electrons e^C , hot electrons e^H
 - argon atoms $Ar(3s^23p^6)$, warm argon atoms in the ground state Ar^W , hot argon atoms in the ground state Ar^H , Ar^m ($1s_5$ and $1s_3$) (11.6 eV), argon ions Ar^+ (15.76 eV)
 - titanium atoms $Ti(a^3F)$, titanium ions Ti^+ (6.83 eV), doubly ionized titanium ions Ti^{2+} (13.58 eV)
 - aluminium atoms $Al(^2P_{1/2})$, aluminium ions Al^+ (5.99 eV), doubly ionized aluminium ions Al^{2+} (18.8 eV)

Detailed model description is given in Huo et al. (2017) JPD **50** 354003



Ionization region model non-reactive HiPIMS

- The particle balance equation for a particular species is given by

$$\frac{dn_{\text{species}}}{dt} = \sum R_{\text{species,process}}$$

- The reaction rate $R_{j,\text{volume}}$ for a given volume reaction of a species j is

$$R_{j,\text{volume}} = k \times \prod_i n_{r,i} \quad [\text{m}^{-3}\text{s}^{-1}]$$

- The rate at which species are sputtered off the target (Al, Ti and O) is

$$R_{n,\text{sputt}} = \frac{\sum_i \Gamma_i^{\text{RT}} S_{\text{RT}} Y_i(\mathcal{E})}{V_{\text{IR}}}$$

and i stands for the ion involved in the process, here $i = \text{Al}^+, \text{Al}^{2+}, \text{Ti}^+, \text{Ti}^{2+}, \text{Ar}^+, \text{O}^+, \text{and } \text{O}_2^+$, Γ_i^{RT} is the flux of ion i towards the target



Ionization region model non-reactive HiPIMS

- For each ion there is a loss rate given as

$$R_{i,\text{loss}} = - \frac{\Gamma_i^{\text{BP}} S_{\text{BP}} + \Gamma_i^{\text{RT}} S_{\text{RT}}}{V_{\text{IR}}}$$

where i stands for the particular ion and S_{BP} is the area of the annular cylinder facing the lower density plasma outside the IR (bulk plasma), and Γ_i^{BP} is the flux of ion i across the boundary towards the lower density plasma

- Thus the flux out of the IR towards the lower density plasma is reduced as required to obtain the assumed ion back-attraction probability β

$$\Gamma_i^{\text{BP}} = \left(\frac{1}{\beta} - 1 \right) \frac{S_{\text{IR}}}{S_{\text{BP}}} \Gamma_i^{\text{RT}}$$



Ionization region model non-reactive HiPIMS

- Gas rarefaction lowers the density of the working gas inside the IR below the value in the surrounding gas reservoir, $n_{g,0}$
- This gives a back-diffusion (gain) term

$$R_{g,\text{refill}} = \frac{1}{2} v_{\text{ran}} \frac{(n_{g,0} - n_g) S_{\text{RT}}}{V_{\text{IR}}}$$

where the subscript g stands for the atoms and molecules of the working gas Ar and O₂



Ionization region model non-reactive HiPIMS

- The return flux of recombined positive argon ions Ar^+ from the target is treated as two groups of atoms with different temperatures
 - a hot component Ar^{H} that returns from the target with a typical sputter energy of a few electron volts
 - a warm component Ar^{W} that is assumed to be embedded in the target at the ion impact, and then return to the surface and finally leave with the target temperature, at most 0.1 eV
- Thus there is a loss out of the IR

$$R_{\text{Ar}^Z, \text{loss}} = -v_{\text{ran}} n_{\text{Ar}^Z} \frac{S_{\text{RT}}}{V_{\text{IR}}}$$

where Z stands for H for hot or W for warm argon atoms



Ionization region model non-reactive HiPIMS

- In addition there is a change in the neutral density due to kick-out by collisions with fast sputtered atoms coming from the target
- For each of the neutrals Y of the working gas, including each of the metastable states, the particle balance includes a loss term

$$R_{n,\text{kick-out}} = -\frac{1}{2} \frac{v_{\text{ran},X}}{L} F_{\text{coll}} \frac{M_X}{M_Y} \frac{\sum_i n_{X,i}}{\sum_i n_{Y,i}} n_Y$$

- The sum is taken over all the states of that sputtered species and

$$F_{\text{coll}} = 1 - \exp(-L/\lambda_{X,\text{gas}})$$

is the probability of a collision inside the IR, where $\lambda_{X,\text{gas}}$ is the mean free path for an atom X sputtered off the target

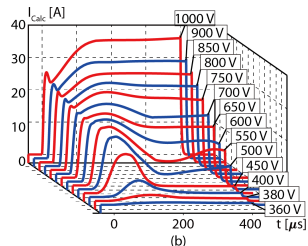
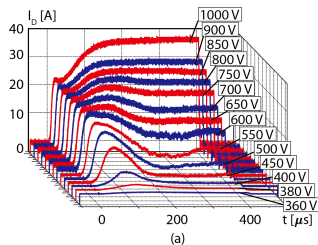


Ionization region model non-reactive HiPIMS

- The IRM is a semi-empirical model in the sense that it uses a measured discharge current waveform as a main input parameter
- Measured and calculated temporal variations of the discharge current for various discharge (cathode) voltages for a 50 mm diameter Al target

From Huo et al. (2017) JPD **50** 354003

Experimental data from Anders et al. (2007) JAP **102** 113303

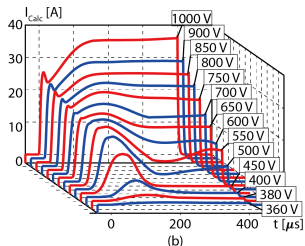
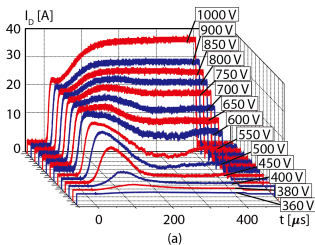


Ionization region model non-reactive HiPIMS

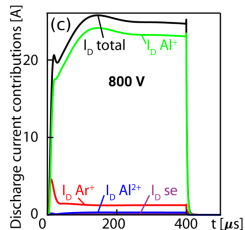
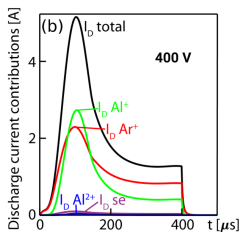
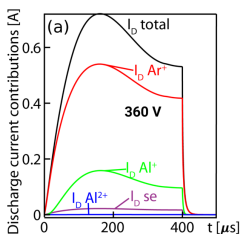
- The model needs to be adapted to an existing discharge (the geometry and pressure, the process gas, sputter yields, target species, and a reaction set for these species) and then fitted to two or three parameters
 - The voltage drop across the IR, V_{IR} , accounts for the power transfer to the electrons
 - The probability of back-attraction of ions to the target β
 - The probability r of back-attraction of secondary electrons emitted

From Huo et al. (2017) JPD **50** 354003

Experimental data from Anders et al. (2007) JAP **102** 113303



Ionization region model of HiPIMS



- A **non-reactive** discharge with 50 mm diameter Al target
- Current composition at the target surface

From Huo et al. (2017) JPD **50** 354003

Experimental data from Anders et al. (2007) JAP **102** 113303

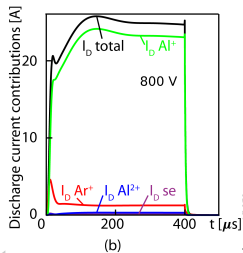
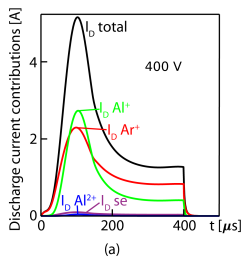


Ionization region model non-reactive HiPIMS

- A **non-reactive** discharge with Al target
- When the discharge is operated at 400 V the contributions of Al^+ and Ar^+ -ions to the discharge current are very similar
- At 800 V Al^+ -ions dominate the discharge current (**self-sputtering**) while the contribution of Ar^+ is below 10 % except at the initiation of the pulse

From Huo et al. (2017) JPD **50** 354003

Experimental data from Anders et al. (2007) JAP **102** 113303

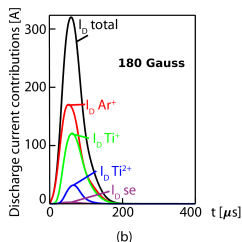
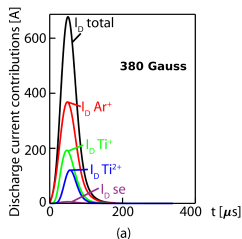


Ionization region model non-reactive HiPIMS

- A **non-reactive** discharge with Ti target
- The contributions to the discharge current for two cases, weak (180 Gauss) and strong (380 Gauss) magnetic field, at 75 Hz pulse frequency
- Stronger magnetic field leads to a higher discharge current
- Higher magnetic field strength leads to higher relative contribution of Ti^{2+} while it lowers the relative contribution of Ti^{+}

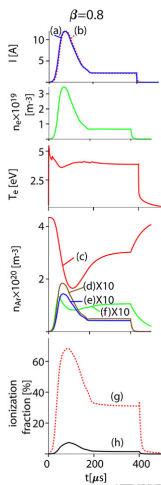
From Huo et al. (2017) JPD **50** 354003

Experimental data from Bradley et al. (2015) JPD **48** 215202



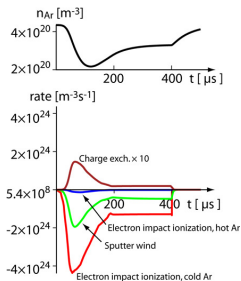
Ionization region model non-reactive HiPIMS

- Discharge operated in argon at 1.8 Pa with a 2 inch Al target, with a pulse voltage of 450 V and a peak discharge current of 12 A
- The discharge current (a) experimentally recorded and (b) calculated
- Electron density and electron temperature
 - (c) argon working gas density
 - (d) argon ion density n_{Ar^+} ,
 - (e) hot recombined argon density n_{Ar^H}
 - (f) metastable argon density n_{Ar^m}
 - (g) ionized density fraction of the sputtered species (aluminum), $F_{density,Al}$
 - (h) ionized density fraction of the argon working gas, $F_{density,Ar}$



Ionization region model non-reactive HiPIMS

- One important process is gas rarefaction, which results in a depletion of the working gas density in the near-cathode region
- The rate of gas rarefaction dn_{Ar}/dt is the fastest at the maximum in discharge current, and a highest absolute value of the gas rarefaction $\Delta n_{Ar}/n_{Ar,0} \approx 50\%$ (top black curve) appears 40 – 60 μs after the discharge current maximum
- After the pulse is turned off ($t = 400 \mu s$) the gas refills and, with a time constant of 100 – 120 μs , returns to the initial value $n_{Ar,0}$

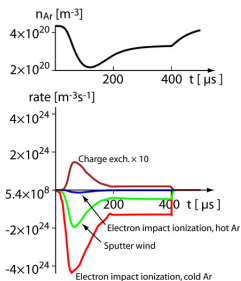


From Huo et al. (2012) PSST 21 045004



Ionization region model non-reactive HiPIMS

- The processes that make contribution to gas rarefaction in a HiPIMS discharge with argon as working gas at 1.8 Pa, Al target and $V_D = 450$ V
- The dominating loss terms are
 - electron impact ionization
 - sputter wind kick-out
- The ionization term is larger by more than a factor of two throughout the pulse
- Most of the sputter wind would therefore pass through the dense ionization region without colliding with a working gas atom



From Huo et al. (2012) PSST 21 045004

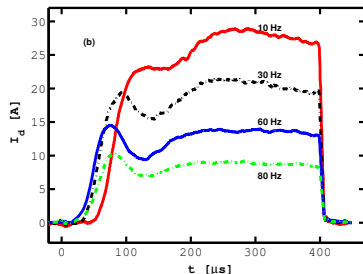
Voltage - Current - Time characteristics

Reactive HiPIMS



HiPIMS - Voltage - Current - time

- During **reactive sputtering**, a reactive gas is added to the inert working gas
- The current waveform in the reactive Ar/N₂ HiPIMS discharge with Ti target is highly dependent on the pulse repetition frequency
- N₂ addition changes the plasma composition and the target condition can also change due to the formation of a compound on its surface

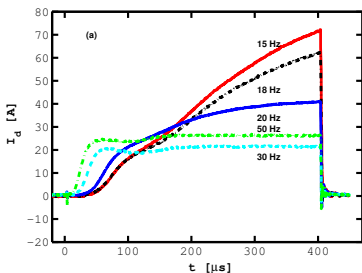


After Magnus et al. (2011) JAP **110** 083306



HiPIMS - Voltage - Current - time

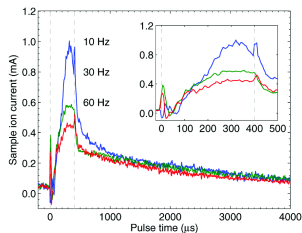
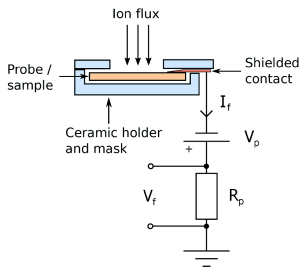
- Similarly for the Ar/O₂ discharge, the current waveform is highly dependent on the repetition frequency and applied voltage which is linked to oxide formation on the target
- The current is found to increase significantly as the frequency is lowered and develop a triangular shape



After Magnus et al. (2012) JVSTA **30** 050601

HiPIMS - Voltage - Current - time

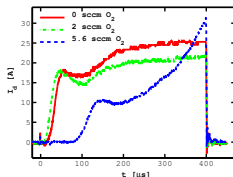
- The observed changes in the discharge current are reflected in the flux of ions impinging on the substrate



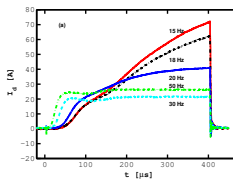
From Magnus et al. (2011) JAP **110** 083306

HiPIMS - Voltage - Current - time

- During **reactive sputtering**, a reactive gas is added to the inert working gas and a transition to oxide mode is observed
- Ar/O₂ discharge with titanium target, pressure 0.6 Pa, and the pulse voltage is 600 V
- The discharge current decreases when 2 sccm and increases as 5.6 sccm of oxygen is added to the discharge
- The current is found to increase significantly as the frequency is lowered



Gudmundsson (2016) PPCF **58** 014002



Magnus et al. (2012) JVSTA **30** 050601



Ionization region model studies of reactive HiPIMS



Ionization region model studies of reactive HiPIMS

- The species assumed in the reactive-IRM are
 - cold electrons e^C , hot electrons e^H
 - argon atoms $Ar(3s^23p^6)$, warm argon atoms in the ground state Ar^W , hot argon atoms in the ground state Ar^H , Ar^m ($1s_5$ and $1s_3$) (11.6 eV), argon ions Ar^+ (15.76 eV)
 - titanium atoms $Ti(a^3F)$, titanium ions Ti^+ (6.83 eV), doubly ionized titanium ions Ti^{2+} (13.58 eV)
 - oxygen molecule in the ground state $O_2(X^3\Sigma_g^-)$, the metastable oxygen molecules $O_2(a^1\Delta_g)$ (0.98 eV) and $O_2(b^1\Sigma_g)$ (1.627 eV), the oxygen atom in the ground state $O(^3P)$, the metastable oxygen atom $O(^1D)$ (1.96 eV), the positive ions O_2^+ (12.61 eV) and O^+ (13.62 eV), and the negative ion O^-

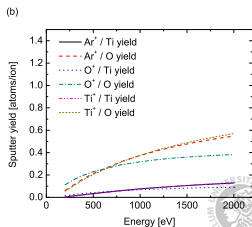
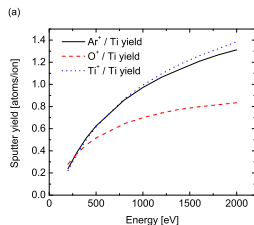
Toneli et al. (2015) J. Phys. D. **48** 325202

Gudmundsson et al. (2016) PSST **25**(6) 065004



Ionization region model studies of reactive HiPIMS

- The sputter yield for the various bombarding ions was calculated by TRIDYN for
 - **Metal mode** – Ti target
 - **Poisoned mode** – TiO₂ target
- The sputter yields correspond to the extreme cases of either clean Ti surface and a surface completely oxidized (TiO₂ surface)
- The sputter yield is much lower for poisoned target

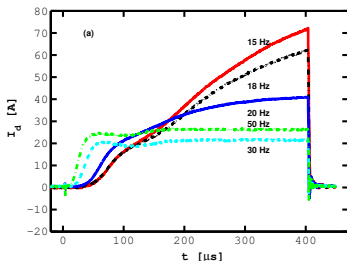


The sputter yield data is from Tomáš Kubart, Uppsala University



Ionization region model studies of reactive HiPIMS

- The model is applied to explore Ar/O₂ discharge with Ti target in both metal mode and oxide (poisoned) mode
- The IRM is a semi-empirical model in the sense that it uses a measured discharge voltage and current waveforms as a main input parameter
- For this study we use the measured curve for Ar/O₂ with Ti target at 50 Hz for metal mode and at 15 Hz for poisoned mode

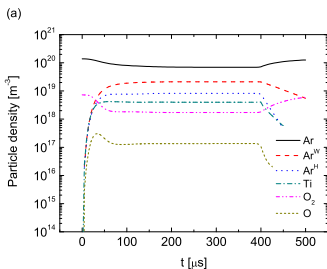


After Magnus et al. (2012) JVSTA **30** 050601



Ionization region model studies of reactive HiPIMS

- The gas rarefaction is observed for the argon atoms but is more significant for the O_2 molecule
- The density of Ti atoms is higher than the O_2 density
- The atomic oxygen density of is over one order of magnitude lower than the molecular oxygen density – the dissociation fraction is low



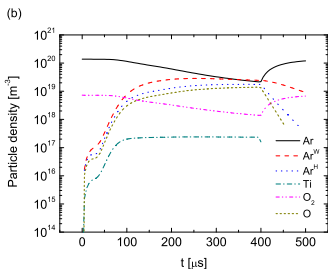
The temporal evolution of the neutral species with 5 % oxygen partial flow rate for Ar/ O_2 discharge with Ti target in **metal mode**.

Gudmundsson et al. (2016) PSST 25(6) 065004



Ionization region model studies of reactive HiPIMS

- Gas rarefaction is observed for both argon atoms and O₂ molecules
- The density of Ti atoms is lower than both the O₂ density and atomic oxygen density
- The atomic oxygen density is higher than the O₂ density towards the end of the pulse



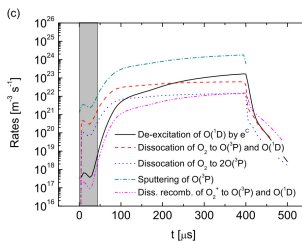
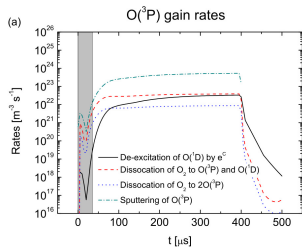
The temporal evolution of the neutral species with 5 % oxygen partial flow rate for Ar/O₂ discharge with Ti target in **poisoned mode**.

Ionization region model studies of reactive HiPIMS

- The increase in the atomic oxygen in the ground state is due to:
 - sputtering of $O(^3P)$ from the partially to fully oxidized target (dominates)
 - electron impact de-excitation of $O(^1D)$
 - electron impact dissociation of the O_2 ground state molecule

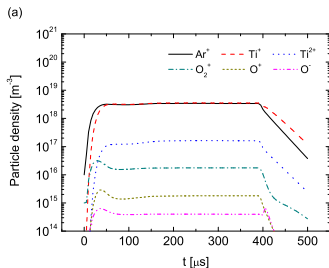
The temporal evolution of the neutral species with **5 % oxygen partial flow rate** for Ar/ O_2 discharge with Ti target in **transition mode** and **poisoned mode**.

Lundin et al. (2017) JAP 121(17) 171917



Ionization region model studies of reactive HiPIMS

- In **metal mode** Ar^+ and Ti^+ -ions dominate the discharge
- Ti^{2+} -ions follow by roughly an order of magnitude lower density
- The O_2^+ and O^+ -ion density is much lower



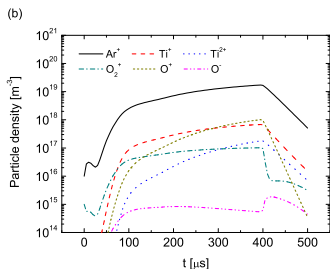
The temporal evolution of the neutral species with **5 % oxygen partial flow rate** for Ar/O_2 discharge with Ti target in **metal mode**.

Gudmundsson et al. (2016) PSST 25(6) 065004



Ionization region model studies of reactive HiPIMS

- In **poisoned mode** Ar^+ -ions dominate the discharge
- Ti^+ , O^+ , have very similar density, but the temporal variation is different, and the O_2^+ density is slightly lower
- The Ti^{2+} -ion density increases fast with time and overcomes the O_2^+ density towards the end of the pulse



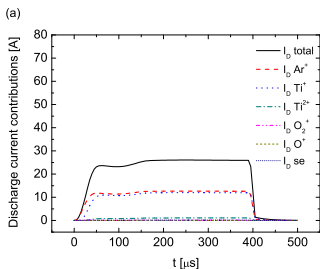
The temporal evolution of the neutral species with 5 % oxygen partial flow rate for Ar/O_2 discharge with Ti target in **poisoned mode**.

Gudmundsson et al. (2016) PSST 25(6) 065004



Ionization region model studies of reactive HiPIMS

- In **metal mode** Ar^+ and Ti^+ -ions contribute most significantly to the discharge current at the cathode target surface – almost equal contribution

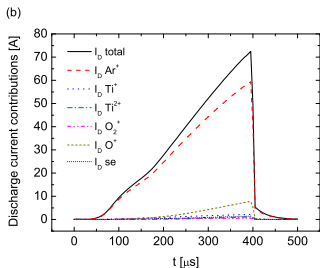


The temporal evolution of the neutral species with **5 % oxygen partial flow rate** for Ar/O_2 discharge with Ti target in **metal mode**.

Gudmundsson et al. (2016) PSST 25(6) 065004

Ionization region model studies of reactive HiPIMS

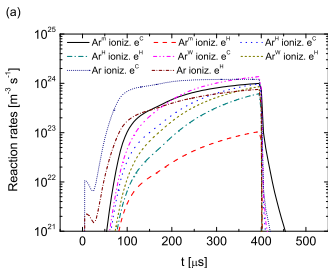
- In **poisoned mode** Ar^+ contribute most significantly to the discharge current – almost solely – at the cathode target surface
- The contribution of secondary electron emission is very small



The temporal evolution of the neutral species with **5 % oxygen partial flow rate** for Ar/O_2 discharge with Ti target in **poisoned mode**.

Ionization region model studies of reactive HiPIMS

- Recycling of atoms coming from the target and then ionized are required for the current generation in both modes of operation
- In the metal mode self-sputter recycling dominates and in the poisoned mode working gas recycling dominates
- The dominating type of recycling determines the discharge current waveform



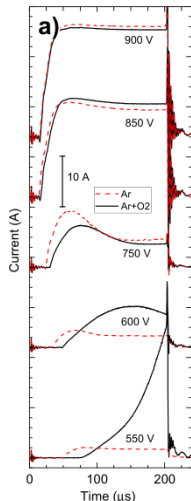
The temporal variations of the reaction rates for electron impact ionization of the argon atoms (ground state plus metastable) in poisoned mode.

Gudmundsson et al. (2016) PSST 25(6) 065004



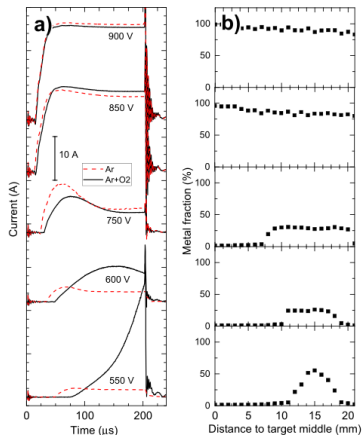
Ionization region model studies of reactive HiPIMS

- The transition to continuously increasing triangular-shaped has been observed experimentally for a Cr target operated in an Ar/O₂ mixture
- Using *in situ* spatially resolved XPS the surface composition of the Cr target was recorded
- Only when the target race track was completely covered by an oxide layer, the triangular pulse shape is observed
- In all other cases, a plateau current was observed



Ionization region model studies of reactive HiPIMS

- If at least 20% of the target area is metallic, then metal atom recycling dominates and a plateau current is observed
- Discharge current waveforms for different applied voltages at discharge frequency of 20 Hz, without and with 0.4% O₂ in the gas mixture
- The profiles of the atomic metal fraction (at%) along the radius of the targets



The generalized recycling model

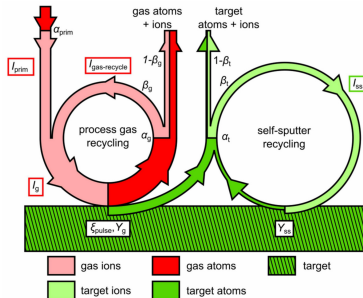


Generalized recycling

- We have seen that the discharge current is composed of
 - working gas ions
 - ions of the sputtered material
- The total discharge current is

$$I_D = I_{\text{prim}} + I_{\text{gas-recycle}} + I_{\text{SS}}$$

- We have also seen that a large fraction of these ions have to be recycled



From Brenning et al. (2017) PSST 26 125003

Generalized recycling

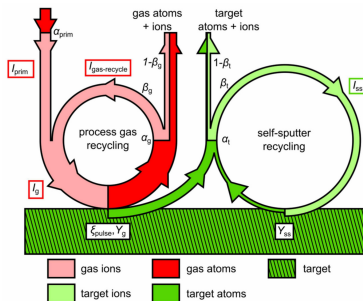
- A working gas-sputtering parameter

$$\pi_g = \alpha_g \beta_g \xi_{\text{pulse}}$$

where

- α_g is ionization probability
 - β_g is back attraction probability
 - $\xi_{\text{pulse}} = 1$ is return fraction in a pulse
- The total current carried by working gas ions

$$I_g = I_{\text{prim}} + I_{\text{gas-recycle}} = I_{\text{prim}} \left(1 + \frac{\pi_g}{1 - \pi_g} \right)$$



From Brenning et al. (2017) PSST 26 125003

Generalized recycling

- The total self-sputter current is

$$I_{SS} = I_g \left(\frac{Y_g}{Y_{SS}} \frac{\pi_{SS}}{1 - \pi_{SS}} \right)$$

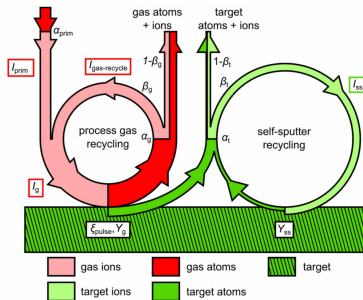
where the self-sputter parameter is

$$\pi_{SS} = \alpha_t \beta_t Y_{SS}$$

- The total discharge current is

$$I_D = I_{\text{prim}} + I_{\text{gas-recycle}} + I_{SS}$$

$$= I_{\text{prim}} \left(1 + \frac{\pi_g}{1 - \pi_g} \right) \left(1 + \frac{Y_g}{Y_{SS}} \frac{\pi_{SS}}{1 - \pi_{SS}} \right)$$



From Brenning et al. (2017) PSST 26 125003.

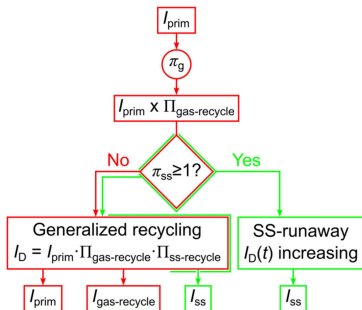


Generalized recycling

- The discharge current

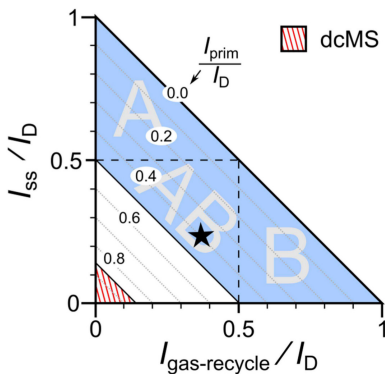
$$I_D = I_{\text{prim}} \Pi_{\text{gas-recycle}} \Pi_{\text{SS-recycle}}$$

- I_{prim} is the seed current that acts as a seed to the whole discharge current and has an upper limit I_{crit}
- $I_{\text{prim}} \Pi_{\text{gas-recycle}}$ is the seed current for the self-sputter process
- If $\pi_{\text{SS}} > 1$ the discharge goes into SS-runaway



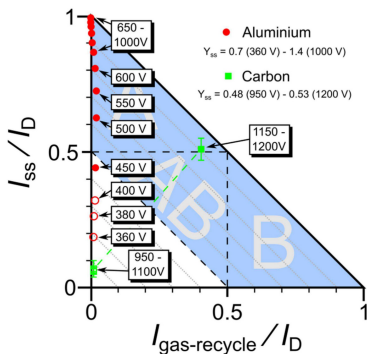
Generalized recycling

- Recycling map
- A graph in which the ion current mix of I_{prim} , $I_{\text{gas-recycle}}$, and I_{SS} to the target in a magnetron discharge is defined by a point
- The value of $I_{\text{prim}}/I_{\text{D}} = 39\%$, can be read on the diagonal lines ($Y_{\text{SS}} = 0.5$)
- $I_{\text{prim}}/I_{\text{D}} \geq 0.85$ defines the dcMS regime
- For $I_{\text{SS}}/I_{\text{D}} > 0.5$ we have the SS-recycle dominated range A
- For $I_{\text{gas-recycle}}/I_{\text{D}} > 0.5$ we have the gas-recycle dominated range B



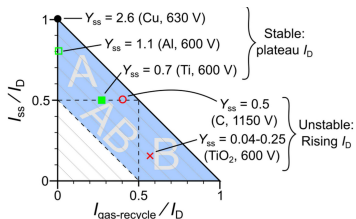
Generalized recycling

- The discharge with Al target moves from the dcMS regime to the HiPIMS discharge regime with increased discharge voltage – **type A**
- A discharge with carbon target jumps from the dcMS regime to the HiPIMS regime – both SS recycling and working gas recycling play a role – intermediate **type AB**



Generalized recycling

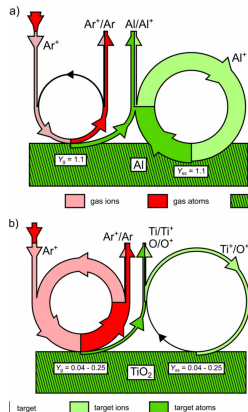
- Recycling map for five different targets with varying self-sputter yield
 - Cu – $Y_{SS} = 2.6$
 - Al – $Y_{SS} = 1.1$
 - Ti – $Y_{SS} = 0.7$
 - C – $Y_{SS} = 0.5$
 - TiO_2 – $Y_{SS} = 0.04 - 0.25$
- For very high self-sputter yields $Y_{SS} > 1$, the discharges above I_{crit} are of **type A** with dominating **SS-recycling**
- For very low self-sputter yields $Y_{SS} < 0.2$, the discharges above I_{crit} are of **type B** with dominating **working gas recycling**



From Brenning et al. (2017) PSST **26** 125003

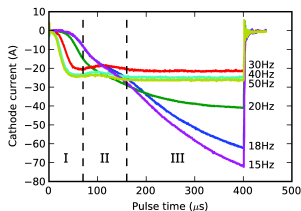
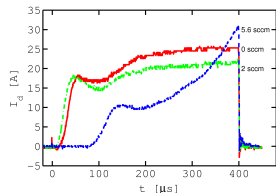
Generalized recycling

- Recycling loops
- Discharge with Al target – SS recycling dominates
 - high self sputter yield
- Reactive discharge with TiO_2 target – working gas recycling dominates
 - low self sputter yield



HiPIMS - Voltage - Current - time

- For Ar/O₂ discharge with Ti target
- At high frequencies, oxide is not able to form between pulses, and **self-sputtering recycling** by Ti⁺-ions is the dominant process
- At low frequency, the long off-time results in an oxide layer being formed (TiO₂) on the target surface and **working gas recycling dominates** – triangular current waveform



Summary



Summary

- The current-voltage-time waveforms in a reactive discharge exhibit similar general characteristics as the non-reactive case in some cases
 - the current rises to a peak, then decays because of rarefaction before rising to a self-sputtering dominated phase
 - in other cases the current develops a triangular shape as repetition frequency is lowered or the partial pressure of the reactive gas is increased
- The secondary electron emission yield is higher for a nitride or oxide target than a titanium target when self-sputtering is the dominant sputtering mechanism



Summary

- An ionization region model was used to explore the plasma composition during the high power pulse
- Comparison was made between the metal mode and the poisoned mode
 - In metal mode Ar^+ and Ti^+ -ions dominate the discharge and are of the same order of magnitude
 - In poisoned mode Ar^+ -ions dominate the discharge and two orders of magnitude lower, Ti^+ , O^+ , have very similar density, with the O_2^+ density slightly lower
 - In the metal mode Ar^+ and Ti^+ -ions contribute most significantly to the discharge current while in poisoned mode Ar^+ dominate
- In the metal mode self-sputter recycling dominates and in the poisoned mode working gas recycling dominates – the dominating type of recycling determines the discharge current waveform



The slides can be downloaded at

<http://langmuir.raunvis.hi.is/~tumi/ranns.html>

- The work is in collaboration with
 - Dr. Daniel Lundin, Université Paris-Sud, Orsay, France
 - Prof. Nils Brenning, KTH Royal Institute of Technology, Stockholm, Sweden
 - Dr. Michael A. Raadu, KTH Royal Institute of Technology, Stockholm, Sweden
 - Prof. Tiberu Minea, Université Paris-Sud, Orsay, France
- We got help with the sputtering yields from
 - Dr. Tomas Kubart, Uppsala University, Uppsala, Sweden
- and the project has been funded by
 - Icelandic Research Fund Grant No. 130029 and 196141
 - Swedish Government Agency for Innovation Systems (VINNOVA) contract no. 2014-04876,



References

- Agnarsson, B., F. Magnus, T. K. Tryggvason, A. S. Ingason, K. Leosson, S. Olafsson, and J. T. Gudmundsson (2013). Rutile TiO₂ thin films grown by reactive high power impulse magnetron sputtering. *Thin Solid Films* 545, 445–450.
- Alami, J., P. O. A. Petersson, D. Music, J. T. Gudmundsson, J. Bohlmark, and U. Helmersson (2005). Ion-assisted physical vapor deposition for enhanced film deposition on non-flat surfaces. *Journal of Vacuum Science and Technology A* 23(2), 278–280.
- Anders, A., J. Andersson, and A. Ehasarian (2007). High power impulse magnetron sputtering: Current-voltage-time characteristics indicate the onset of sustained self-sputtering. *Journal of Applied Physics* 102(11), 113303.
- Bohlmark, J., J. T. Gudmundsson, J. Alami, M. Lattemann, and U. Helmersson (2005). Spatial electron density distribution in a high-power pulsed magnetron discharge. *IEEE Transactions on Plasma Science* 33(2), 346–347.
- Bradley, J. W., A. Mishra, and P. J. Kelly (2015). The effect of changing the magnetic field strength on HiPIMS deposition rates. *Journal of Physics D: Applied Physics* 48(21), 215202.
- Brenning, N., J. T. Gudmundsson, M. A. Raadu, T. J. Petty, T. Minea, and D. Lundin (2017). A unified treatment of self-sputtering, process gas recycling, and runaway for high power impulse sputtering magnetrons. *Plasma Sources Science and Technology* 26(12), 125003.
- Gudmundsson, J. T. (2008). Ionized physical vapor deposition (IPVD): Magnetron sputtering discharges. *Journal of Physics: Conference Series* 100, 082002.
- Gudmundsson, J. T. (2016). On reactive high power impulse magnetron sputtering. *Plasma Physics and Controlled Fusion* 58(1), 014002.
- Gudmundsson, J. T. (2020). Physics and technology of magnetron sputtering discharges. *Plasma Sources Science and Technology* 29.
- Gudmundsson, J. T., N. Brenning, D. Lundin, and U. Helmersson (2012). The high power impulse magnetron sputtering discharge. *Journal of Vacuum Science and Technology A* 30(3), 030801.
- Gudmundsson, J. T. and D. Lundin (2020). Introduction to magnetron sputtering. In D. Lundin, T. Minea, and J. T. Gudmundsson (Eds.), *High Power Impulse Magnetron Sputtering: Fundamentals, Technologies, Challenges and Applications*, pp. 1–48. Amsterdam, The Netherlands: Elsevier.

References

- Gudmundsson, J. T., D. Lundin, N. Brenning, M. A. Raadu, C. Huo, and T. M. Minea (2016). An ionization region model of the reactive Ar/O₂ high power impulse magnetron sputtering discharge. *Plasma Sources Science and Technology* 25(6), 065004.
- Hajihoseini, H. and J. T. Gudmundsson (2017). Vanadium and vanadium nitride thin films grown by high power impulse magnetron sputtering. *Journal of Physics D: Applied Physics* 50(50), 505302.
- Huo, C., D. Lundin, J. T. Gudmundsson, M. A. Raadu, J. W. Bradley, and N. Brenning (2017). Particle-balance models for pulsed sputtering magnetrons. *Journal of Physics D: Applied Physics* 50(35), 354003.
- Huo, C., M. A. Raadu, D. Lundin, J. T. Gudmundsson, A. Anders, and N. Brenning (2012). Gas rarefaction and the time evolution of long high-power impulse magnetron sputtering pulses. *Plasma Sources Science and Technology* 21(4), 045004.
- Kateb, M., H. Hajihoseini, J. T. Gudmundsson, and S. Ingvarsson (2019). Role of ionization fraction on the surface roughness, density, and interface mixing of the films deposited by thermal evaporation, dc magnetron sputtering, and HiPIMS: An atomistic simulation. *Journal of Vacuum Science and Technology A* 37(3), 031306.
- Layes, V., C. C. Roca, S. Monje, V. Schulz-von der Gathen, A. von Keudell, and T. de los Arcos (2018). Connection between target poisoning and current waveforms in reactive high power impulse magnetron sputtering of chromium. *Plasma Sources Science and Technology* 27(8), 084004.
- Leosson, K., S. Shayestehaminzadeh, T. K. Tryggvason, A. Kossov, B. Agnarsson, F. Magnus, S. Olafsson, J. T. Gudmundsson, E. B. Magnusson, and I. A. Shelykh (2012). Comparing resonant photon tunneling via cavity modes and Tamm plasmon polariton modes in metal-coated Bragg mirrors. *Optics Letters* 37(19), 4026–4028.
- Lundin, D., J. T. Gudmundsson, N. Brenning, M. A. Raadu, and T. M. Minea (2017). A study of the oxygen dynamics in a reactive Ar/O₂ high power impulse magnetron sputtering discharge using an ionization region model. *Journal of Applied Physics* 121(17), 171917.
- Magnus, F., A. S. Ingason, S. Olafsson, and J. T. Gudmundsson (2012). Nucleation and resistivity of ultrathin TiN films grown by high power impulse magnetron sputtering. *IEEE Electron Device Letters* 33(7), 1045 – 1047.



References

- Magnus, F., O. B. Sveinsson, S. Olafsson, and J. T. Gudmundsson (2011). Current-voltage-time characteristics of the reactive Ar/N₂ high power impulse magnetron sputtering discharge. *Journal of Applied Physics* 110(8), 083306.
- Magnus, F., T. K. Tryggvason, S. Olafsson, and J. T. Gudmundsson (2012). Current-voltage-time characteristics of the reactive Ar/O₂ high power impulse magnetron sputtering discharge. *Journal of Vacuum Science and Technology A* 30(5), 050601.
- Raadu, M. A., I. Axnäs, J. T. Gudmundsson, C. Huo, and N. Brenning (2011). An ionization region model for high power impulse magnetron sputtering discharges. *Plasma Sources Science and Technology* 20(6), 065007.
- Samuelsson, M., D. Lundin, J. Jensen, M. A. Raadu, J. T. Gudmundsson, and U. Helmersson (2010). On the film density using high power impulse magnetron sputtering. *Surface and Coatings Technology* 202(2), 591–596.
- Toneli, D. A., R. S. Pessoa, M. Roberto, and J. T. Gudmundsson (2015). On the formation and annihilation of the singlet molecular metastables in an oxygen discharge. *Journal of Physics D: Applied Physics* 48(32), 325202.

